Computational model of minimal NCT

R. Andreev, L. Kapinos, R. Y. H. Lim

2022-02-23

1 Introduction

COMPILATION: 2022-02-23

TODO(1): hydrolysis rate!?

TODO(2): what is NCT

TODO(3): who is involved – transport receptors TODO(4): why these transport recp TODO(5): models

TODO(6): contsrut atrificial cells to reproduce a minimalistic NCT system, with the minimal reasonable number of players and to explain observations in vivo showing down or upregulation of certain species TODO(7): the computatino al model, in turn, closely resembles the design of the artificial cell TODO(8): here we want to prove that with those players of NCT, the essential observations from are reproduced

TODO(9): role TODO(10): sys with compartments TODO(11): visual distribution assuming simple system

We are particularly interested in the nuclear-to-cytoplasmic contrast (henceforth, N:C contrast) of certain molecular species at steady state: $\mathsf{Ran \cdot GTP}$, $\mathsf{Imp\beta}$, CAS, and NLS.

TODO(12): ImpBeta = KapBeta1

Abbreviations. FG-nups = FG-nucleoporins; NCT = nucleocytoplasmic transport; NPC = nuclear pore complex; NE = nuclear envelope; IBB = importin beta binding; ODE = ordinary differential equations; SPR = surface plasmon resonance;

2 NCT models

2.1 GSR'03 model of NCT

Ran gradient. The Ran gradient, i.e. the nuclear accumulation of $\mathsf{Ran}\cdot\mathsf{GTP}$, is the base layer of nucleocytoplasmic transport. We implement it as the "minimal Ran gradient system" from [GSR03]. The equations are recapitulated in §3.1 and the constants are collected in Table 2. TODO(13): simplify: Following [GSR03], the "dynamic capacity" Ex is an optional maximal steady-state (positive) flux of nuclear $\mathsf{Ran}\cdot\mathsf{GTP}$ to cytoplasmic $\mathsf{Ran}\cdot\mathsf{GDP}$, which we determine using the additional equation (18). The fluxes are in units of concentration/time (µM/s). The ones across the nuclear boundary have positive sign when exiting the nucleus and are normalized to the nuclear volume. Thus, the *amount* exiting the nucleus per unit of time is $\mathsf{flux}\times V_{\mathrm{nuc}}$.

Simulating the ODE across the scenarios of [GSR03] we obtain results that are sufficiently close to the original, see Table 3. Importantly, an order of 1000-fold nuclear enrichment of $\mathsf{Ran}\cdot\mathsf{GTP}$ is sustained in steady-state. Moreover, the dynamic capacity clocks in at around 0.6 µM/s in most cases, meaning the Ran gradient is established within seconds. Therefore, we will replace the whole Ran gradient layer by a virtual pump

$$\text{cytoplasmic } \mathsf{Ran}\cdot\mathsf{GDP} \longrightarrow \text{nuclear } \mathsf{Ran}\cdot\mathsf{GTP} \quad \text{with kinetic rate } 0.1\,\mathrm{s}^{-1}. \tag{1}$$

This rate is chosen conservatively (a concentration of 1 µM of cytoplasmic $\mathsf{Ran}\cdot\mathsf{GDP}$ generates a flux of 0.1 µM/s) but will be sufficient for our purposes.

Code #1.

Coupling to Impβ-mediated transport. A coupling of the Ran gradient to importin–cargo transport was proposed in [GSR03, Fig. 6A]. TODO(14): do they have a steady-state result TODO(15): kinetic behavior of Imp, in addition to cargo and ran TODO(16): no NE TODO(17): we look at steady-state We now formulate a version of it. The following equations comprise the handling of cargo by $\mathsf{Impβ}$ in the cytoplasm,

$$\tfrac{\mathrm{d}}{\mathrm{d}t}[\mathsf{Impβ}\cdot\mathsf{Ran}\cdot\mathsf{GTP}]_{\mathrm{cyt}} = -\mathsf{R}_{\mathrm{cyt}} + \mathsf{F}_{\mathsf{Impβ}\cdot\mathsf{Ran}\cdot\mathsf{GTP}}\tfrac{V_{\mathrm{nuc}}}{V_{\mathrm{cyt}}} - \mathsf{GAP}_{\mathsf{Impβ}} + \mathsf{Knockoff}_{\mathrm{cyt}} \tag{2a}$$

$$\tfrac{\mathrm{d}}{\mathrm{d}t}[\mathsf{Impβ}]_{\mathrm{cyt}} = +\mathsf{R}_{\mathrm{cyt}} + \mathsf{C}_{\mathrm{cyt}} + \mathsf{F}_{\mathsf{Impβ}}\tfrac{V_{\mathrm{nuc}}}{V_{\mathrm{cyt}}} + \mathsf{GAP}_{\mathsf{Impβ}} \tag{2b}$$

$$\tfrac{\mathrm{d}}{\mathrm{d}t}[\mathsf{Impβ}\cdot\mathsf{Cargo}]_{\mathrm{cyt}} = -\mathsf{C}_{\mathrm{cyt}} + \mathsf{F}_{\mathsf{Impβ}\cdot\mathsf{Cargo}}\tfrac{V_{\mathrm{nuc}}}{V_{\mathrm{cyt}}} - \mathsf{Knockoff}_{\mathrm{cyt}} \tag{2c}$$

$$\tfrac{\mathrm{d}}{\mathrm{d}t}[\mathsf{Cargo}]_{\mathrm{cyt}} = +\mathsf{C}_{\mathrm{cyt}} + \mathsf{F}_{\mathsf{Cargo}}\tfrac{V_{\mathrm{nuc}}}{V_{\mathrm{cyt}}} + \mathsf{Knockoff}_{\mathrm{cyt}} \tag{2d}$$

with the fluxes

$$\mathsf{R}_{\mathrm{cyt}} := -k^{\mathrm{R}}_{\mathrm{on}}[\mathsf{Impβ}][\mathsf{Ran}\cdot\mathsf{GTP}]_{\mathrm{cyt}} + k^{\mathrm{R}}_{\mathrm{off}}[\mathsf{Impβ}\cdot\mathsf{Ran}\cdot\mathsf{GTP}]_{\mathrm{cyt}} \tag{3a}$$

$$\mathsf{C}_{\mathrm{cyt}} := -k^{\mathrm{C}}_{\mathrm{on}}[\mathsf{Impβ}][\mathsf{Cargo}]_{\mathrm{cyt}} + k^{\mathrm{C}}_{\mathrm{off}}[\mathsf{Impβ}\cdot\mathsf{Cargo}]_{\mathrm{cyt}}. \tag{3b}$$

The forward flux of the reaction

$$\mathsf{Imp\beta \cdot Cargo} + \mathsf{Ran \cdot GTP} \rightleftharpoons \mathsf{Imp\beta \cdot Ran \cdot GTP} + \mathsf{Cargo} \tag{4}$$

is called Knockoff. It is modeled as a one-way reaction with forward rate k_{knockoff}. The GSR equations are modified accordingly:

$$\tfrac{\mathrm{d}}{\mathrm{d}t}[\mathsf{Ran \cdot GDP}]_{\text{cyt}} = (12\text{a}) + \mathsf{GAP}_{\mathsf{Imp\beta}} \tag{12a$'$}$$
$$\tfrac{\mathrm{d}}{\mathrm{d}t}[\mathsf{Ran \cdot GTP}]_{\text{cyt}} = (12\text{b}) + \mathsf{R}_{\mathsf{cyt}} - \mathsf{Knockoff}_{\mathsf{cyt}} \tag{12b$'$}$$

Analogous nuclear equations (without GAP) are implemented but are omitted here. Analogously to (16a)/(16b) we have the additional nuclear-to-cytoplasmic diffusion fluxes

$$\mathsf{F}_{\mathsf{Imp\beta \cdot Ran \cdot GTP}}, \quad \mathsf{F}_{\mathsf{Imp\beta}}, \quad \mathsf{F}_{\mathsf{Imp\beta \cdot Cargo}}, \quad \mathsf{F}_{\mathsf{Cargo}} \tag{5}$$

with the permeability constants given in Table 1.

SPR experiments of [Cat+01] indicated that the IBB domain of importin-α binds importin-β and undergoes a conformational change,

$$\mathsf{A} + \mathsf{B} \rightleftharpoons \mathsf{AB} \rightleftharpoons \mathsf{A^*B}. \tag{6}$$

We therefore assume the analogous reaction

$$\mathsf{Cargo} + \mathsf{Imp\beta} \underset{k_{d1}}{\overset{k_{a1}}{\rightleftharpoons}} \mathsf{Cargo \cdot Imp\beta} \underset{k_{d2}}{\overset{k_{a2}}{\rightleftharpoons}} \mathsf{Cargo^* \cdot Imp\beta}. \tag{7}$$

Examples of the kinetic constants are available in [Cat+01, Table I], e.g.,

$$k_{a1} = 0.11\,\mu\text{M}^{-1}\,\text{s}^{-1}, \quad k_{d1} = 0.024\,\text{s}^{-1}, \qquad k_{a2} = 0.024\,\text{s}^{-1}, \quad k_{d2} = 7.4 \times 10^{-4}\,\text{s}^{-1}, \tag{8}$$

for an IBB domain binding to Impβ. The intermediate state in (6) is transient on a moderately relevant time-scale (code #2). Therefore, in the present model we lump the complexed states together and take $k_{\text{on}}^{\text{C}} := k_{a1}$ and $k_{\text{off}}^{\text{C}} := k_{d1}\frac{k_{d2}}{k_{a2}+k_{d2}}$ as the effective kinetic constants for (3b), cf. Table 1.

With the constants from Table 1, the steady-state of the model (reached after some 10^4 s) is reported in Fig. 1. Nuclear accumulation of free cargo is 37-fold. Sensitivity analysis shows that, in relative terms, the final nuclear concentration of free cargo depends most strongly on k_{knockoff}. Doubling k_{knockoff} almost doubles the nuclear concentration. Code #3.

This model predicts a slight accumulation of Imgβ in the nucleus, with $\mathsf{Imp\beta \cdot Ran \cdot GTP}$ contributing most of the excess. We improve on it in §2.3.

TODO(18): fluxes in Fig 1

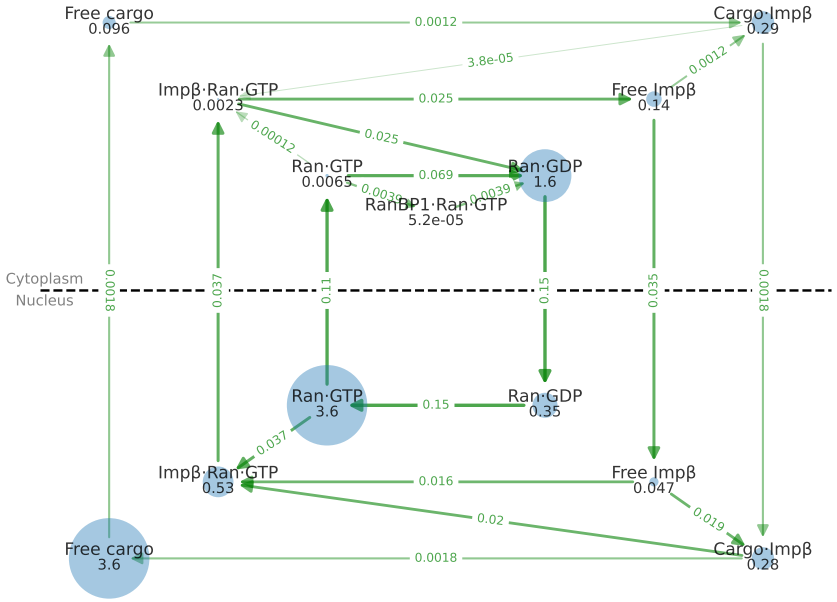

Figure 1: Steady-state of the transport system from §2.1 with conditions of Table 1. The free cargo shows 37-fold accumulation in the nucleus; total nuclear to total cytoplasmic cargo is 10-fold. Units are µM for species and $\mu\mathrm{M\,s^{-1}}$ for fluxes. Initial conditions: $[\mathsf{Ran\cdot GDP}]_{\mathrm{cyt}} = 5\,\mu\mathrm{M}$, $[\mathsf{Imp\beta}]_{\mathrm{cyt}} = 1\,\mu\mathrm{M}$, $[\mathsf{Cargo}]_{\mathrm{cyt}} = 3\,\mu\mathrm{M}$, all else zero.

(3a)	$k_{\mathrm{on}}^{\mathrm{R}} = 0.096\,\mu\mathrm{M}^{-1}\,\mathrm{s}^{-1}$, $k_{\mathrm{off}}^{\mathrm{R}} = 4.8\times10^{-6}\,\mathrm{s}^{-1}$	[GSR03, Supp. Table A], [RM05, Table II]
(3b)	$k_{\mathrm{on}}^{\mathrm{C}} = 0.11\,\mu\mathrm{M}^{-1}\,\mathrm{s}^{-1}$, $k_{\mathrm{off}}^{\mathrm{C}} = 7.2\times10^{-4}\,\mathrm{s}^{-1}$	[Cat+01, Table I], [RM05, Table II]
(4)	$k_{\mathrm{knockoff}} = 2\times10^{-2}\,\mu\mathrm{M}^{-1}\mathrm{s}^{-1}$	[RM05, Table II]
(5)	$D_{\mathsf{Imp\beta\cdot Ran\cdot GTP}} = 0.07\,\mathrm{s}^{-1}$, $D_{\mathsf{Imp\beta}} = 0.4\,\mathrm{s}^{-1}$ $D_{\mathsf{Imp\beta\cdot Cargo}} = 0.25\,\mathrm{s}^{-1}$, $D_{\mathsf{Cargo}} = 5\times10^{-4}\,\mathrm{s}^{-1}$	[RM05, Table III]

Table 1: Constants for the $\mathsf{Imp}\beta$-mediated transport from §2.1.

2.2 GTP hydrolysis and role of RanBP1

According to [LM97, Fig. 4A], Impβ blocks hydrolysis of Ran · GTP by RanGAP but RanBP1 rescues it for most part. Similarly, [BG97] showed that RanBP1 transiently detaches Ran from the complex Kap · Ran · GTP (where Kap is some karyopherin), whereupon hydrolysis by RanGAP disassembles the complex; and that efficient disassembly of Impβ · Ran · GTP required RanBP1 *and* Impα [BG97, §3.2, cf. Fig. 4], [FBR97]. Importantly, Kaps and RanBP1 bind Ran at distinct sites [BG97, p.253].

Further, [See+03, Fig. 13] characterizes the kinetics of the formation of the complex between Ran · GTP, RanBP1 and RanGAP and the hydrolysis. In particular, the release rate of the γ-phosphate, on the order or $10\,\mathrm{s}^{-1}$ in [See+03, Fig. 13], is barely influenced by RanBP1, which instead stimulates the association of Ran with RanGAP. A computational model of hydrolysis with these parameters qualitatively reproduces the experimental data from [LM97, Fig. 4A]. We omit the details that can be found in Code #4.

For simplicity, we will take the constant

$$\text{GTP hydrolysis rate of } 0.1\,\mathrm{s}^{-1} \tag{9}$$

for all cytoplasmic-side species containing Ran · GTP, and no GTP hydrolysis elsewhere. This should be compared with the effective Ran gradient rate (1).

TODO(19): cf [KKL21] citing [Kle+95a] or [Kle+95b]

2.3 NPC as compartment

Introduction. TODO(20): explain initial/final/steady-state

It has been observed [KKL21] that Impβ accumulates inside the NPCs as they bind to the FG-nups, suggesting a regulatory role, and possibly shuttling the cargo across the pore repeatedly. TODO(21): picture To account for this we propose a model with cytoplasm, nucleus and the NPCs as three compartments. The following dual observation is essential (cf. [Hof20]):

1. cytoplasmic and nuclear species initially react with NPC components in proportion to the number of NPCs, and
2. the observed fluorescence signal from Kaps accumulating inside the NPCs scales with the total volume or the capacity of the NPC channel (rather than their number).

The model includes the following main components:

- Impβ (Kapβ1) and the cargo adapter Impα (Kapα). For simplicity, we do not model individual variants or isoforms, cf. [KKL21, p. 2].
- Generic NLS cargo, by itself unable to transition the nuclear envelope efficiently. Requires the Impα to be captured by Impβ.

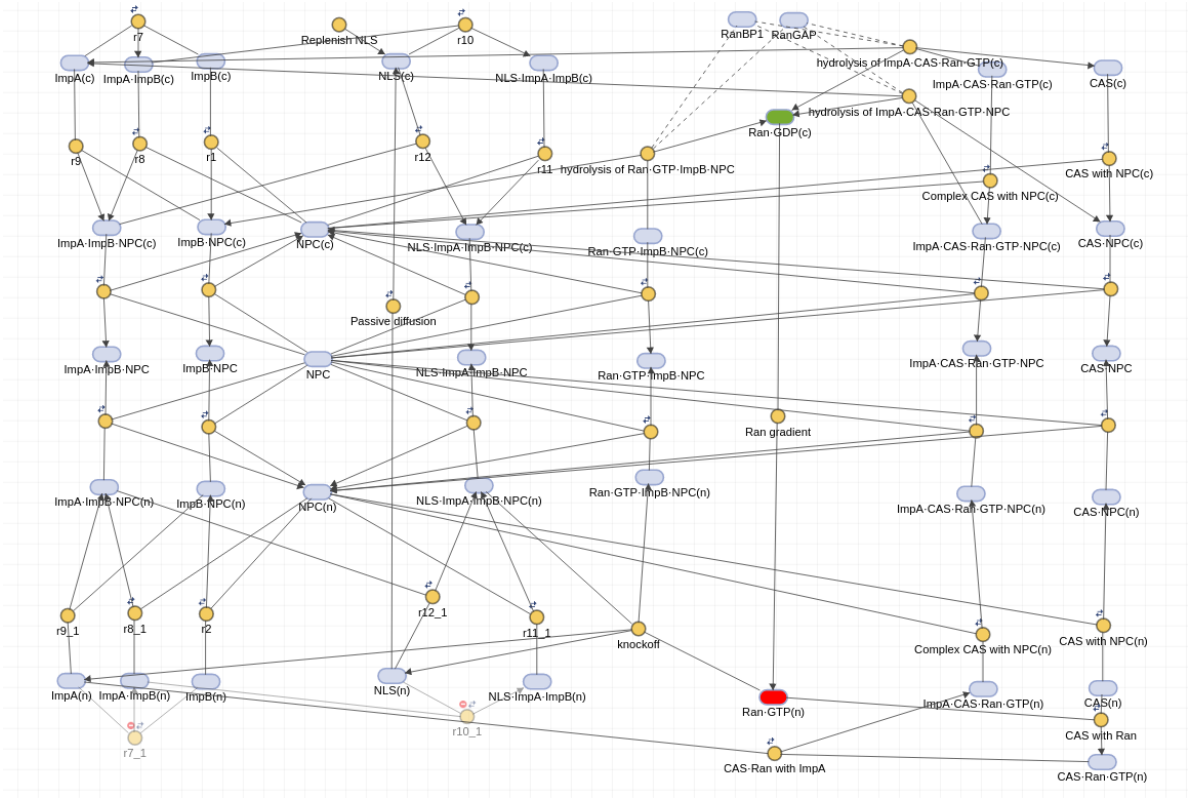

Figure 2: SimBiology diagram for the model "NPC as compartment" from §2.3.

- CAS (Exp2, Xpo2) TODO(22): on CAS
- The NPCs are described as vacant NPC channel space, the cytoplasm-facing opening NPC(c) and the nucleus-facing opening NPC(n). To transition the nuclear pore, a species has to bind to the opening, transition into the channel, bind to the other opening, and unbind on the other side. This allows us to model the capacity of the NPC and the dwelling time (but we make no distinction between different transiting species). There is no directionality, i.e. a species currently residing in the channel is equally likely to bind to either opening next.
- Ran · GTP in the nucleus and Ran · GDP in the cytoplasm. The consumption of Ran · GTP that have transitioned to the cytoplasmic side by hydrolysis is compensated by an effective pump as in (1). The hydrolysis itself is described by one effective kinetic rate as in (9).

An overview of the model is shown in Fig. 2. The code is found in Code #5. The computational results for this model are summarized in Fig. 3. For details visit the URL

https://numpde.github.io/nct1/code/20211018-Appli/checkpoint/20220209-143110/ (10)

Main reactions. Here we comment on the main reactions of the model. For the complete set we refer to Fig. 2 as well as the URL (10).

- The nuclear $\mathsf{Ran \cdot GTP}$ is converted directly to cytoplasmic $\mathsf{Ran \cdot GDP}$ as in Eqn. (1).
- The $\mathsf{Impβ}$ can shuttle on its own through the NPC or in complex with $\mathsf{Impα}$. We assume that the complex does not form on the nuclear side (due to nuclear $\mathsf{Ran \cdot GEF}$, which is not modeled explicitly).
- The cytoplasmic NLS cargo associates with free cytoplasmic $\mathsf{Impα \cdot Impβ}$ before binding to the cytoplasmic side of the NPC, or with those already attached there. Once the complex is shuttled to the nuclear side, the "knockoff" reaction releases the cargo (the suffix $\mathsf{(n)}$ is omitted):

$$\mathsf{Ran \cdot GTP + NLS \cdot Impα \cdot Impβ \cdot NPC \longrightarrow Ran \cdot GTP \cdot Impβ \cdot NPC + Impα + NLS.}$$

  Thereupon, the complex $\mathsf{Ran \cdot GTP \cdot Impβ}$ can transition from the nuclear to the cytoplasmic side to be hydrolized as in Eqn. (9).
- Like $\mathsf{Impβ}$, CAS can shuttle through the NPC. On the nuclear side, it can first bind to $\mathsf{Ran \cdot GTP}$ then form the $\mathsf{Impα \cdot CAS \cdot Ran \cdot GTP}$ complex. This complex can shuttle through the NPC, and it is disassembled on the cytoplasmic side by the hydrolysis reaction (9).

Baseline parameters. Here we comment on the choice of selected model parameters, such as concentrations and kinetic rates. For the complete set see the URL (10).

The nucleus and the cytoplasm each have a volume of 1 pL.

We estimate the total NPC channel capacity as 2000 NPCs per nuclear envelope (BioNumbers #111130) times 300 Kaps per NPC TODO(23): refs for those numbers. Note that

$$1\,\mathrm{pL} \times 1\,\mu\mathrm{M} \approx 300 \times 2000\,\mathrm{units}, \tag{11}$$

which implies a concentration of 1 µM in a computational volume of 1 pL. The computation itself is performed in amounts (rather than concentration), so to convert to apparent concentration of Kaps at the NE we estimate the volume of the NE as 0.01 pL.‘

For the initial concentration of $\mathsf{Impβ}$ we take 5 µM in nucleus and cytoplasm based on [KKL21, Fig. 4] / [NPW19, Fig. 4a].

[YM06]

For the initial concentration of $\mathsf{Impα}$ we considered taking 5 µM throughout the cell, slightly below that of $\mathsf{Impβ}$, based on the immunoblots of [ZAH13, Fig. 7] and the mass spectrometry measurements for KPNAs from [Wüh+14, Table S5]. This corresponds to all isoforms (TODO(24): paralogs?) of Kapα (KPNA2,3,4,6) TODO(25): [unpublished]. However, this

seemed incompatible with other parameters in that the steady state showed unexpected results, e.g. the NLS remained tied to Impα and nearly equipartitioned between nuclear and cytoplasmic sides. We settled on the Impα concentration of 0.5 µM for the baseline model, which is close to isoform Kapα1 (KPNA2). TODO(26): link gene TODO(27): rerun

[KKL21] [Kır+15]

TODO(28): complete section

Variants. We have defined a handful of scenarios to illustrate how parameter choice affects the steady-states. The results are summarized in Fig. 3. All parameter changes are with respected to the baseline scenario, and are reported at the URL (10). TODO(29): : To see the impact of the prameter on the transport and its robustness, possibly mimicking different cell types and disesase

TODO(30): : Decrease can be validated by depletion via siRNA and increase by transfection with a vector that overexpresses the protein.

1. Decrease Impβ tenfold.

   Slighit accumulation in the nucleus

2. Increase the number of NPCs tenfold.

   Observe incrase of Impb contrast at the NE Kalita 2022

3. Increase Impα tenfold.

   Breakdown of transprt..

4. Decrease Impα tenfold.

   Trnasport still works..

5. Turn off Ran · GTP regeneration, starting from the baseline scenario. We obtain a breakdown of N:C contrast for all species, as expected.

TODO(31): artificial cell should reproduce these

References

[Bis+95] F. R. Bischoff, H. Krebber, E. Smirnova, W. Dong, and H. Ponstingl. "Co-activation of RanGTPase and inhibition of GTP dissociation by Ran–GTP binding protein RanBP1". In: *The EMBO Journal* 14.4 (Feb. 1995), pp. 705–715. DOI: 10.1002/j.1460-2075.1995.tb07049.x (cit. on p. 12).

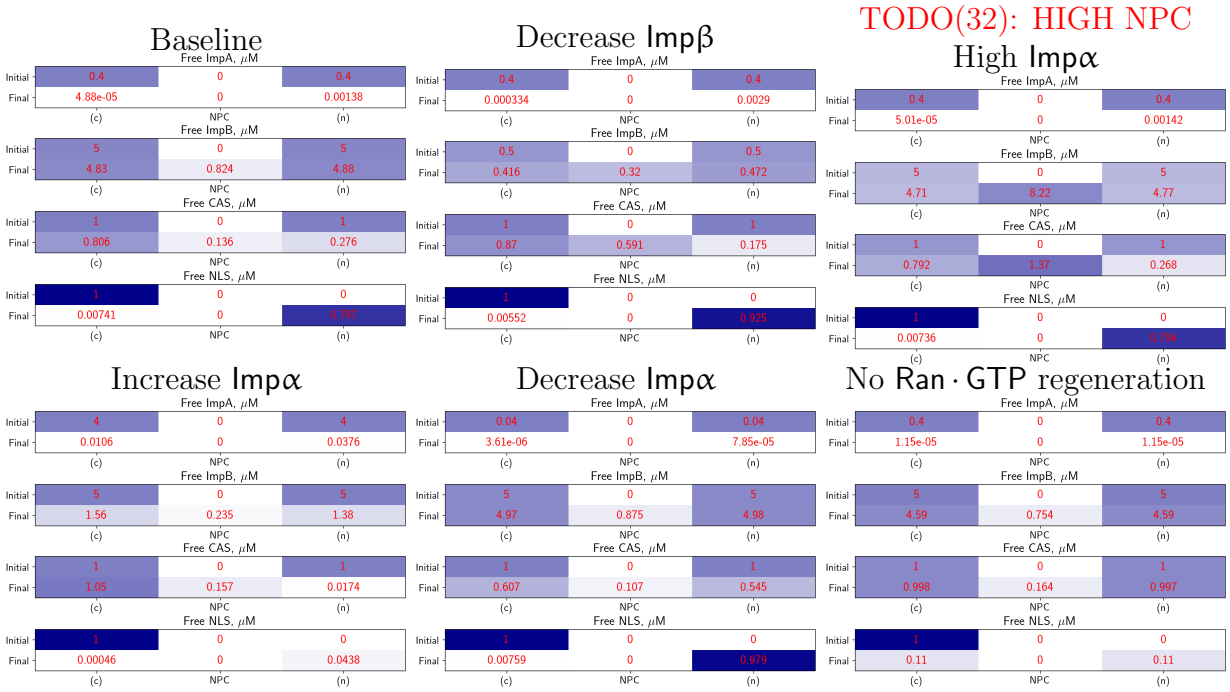

Figure 3: Initial states and steady-states for the model "NPC as compartment" from §2.3. For more full-size figures, see the URL (10).

[Kle+95a] C. Klebe, F. R. Bischoff, H. Ponstingl, and A. Wittinghofer. "Interaction of the Nuclear GTP-Binding Protein Ran with Its Regulatory Proteins RCC1 and RanGAP1". In: *Biochemistry* 34.2 (Jan. 1995), pp. 639–647. DOI: 10.1021/bi00002a031 (cit. on pp. 5, 14).

[Kle+95b] C. Klebe, H. Prinz, A. Wittinghofer, and R. S. Goody. "The Kinetic Mechanism of Ran-Nucleotide Exchange Catalyzed by RCC1". In: *Biochemistry* 34.39 (Oct. 1995), pp. 12543–12552. DOI: 10.1021/bi00039a008 (cit. on pp. 5, 12–14).

[BG97] F. Bischoff and D. Görlich. "RanBP1 is crucial for the release of RanGTP from importin β-related nuclear transport factors". In: *FEBS Letters* 419.2-3 (Dec. 1997), pp. 249–254. DOI: 10.1016/s0014-5793(97)01467-1 (cit. on p. 5).

[FBR97] M. Floer, G. Blobel, and M. Rexach. "Disassembly of RanGTP-Karyopherin β Complex, an Intermediate in Nuclear Protein Import". In: *Journal of Biological Chemistry* 272.31 (Aug. 1997), pp. 19538–19546. DOI: 10.1074/jbc.272.31.19538 (cit. on p. 5).

[LM97] K. M. Lounsbury and I. G. Macara. "Ran-binding Protein 1 (RanBP1) Forms a Ternary Complex with Ran and Karyopherin β and Reduces Ran GTPase-activating Protein (RanGAP) Inhibition by Karyopherin β". In: *Journal of Biological Chemistry* 272.1 (Jan. 1997), pp. 551–555. DOI: 10.1074/jbc.272.1.551 (cit. on p. 5).

[Cat+01] B. Catimel, T. Teh, M. R. Fontes, I. G. Jennings, D. A. Jans, G. J. Howlett, E. C. Nice, and B. Kobe. "Biophysical Characterization of Interactions Involving Importin-α during Nuclear Import". In: *Journal of Biological Chemistry* 276.36 (Sept. 2001), pp. 34189–34198. DOI: 10.1074/jbc.m103531200 (cit. on pp. 3, 4).

[GSR03] D. Görlich, M. J. Seewald, and K. Ribbeck. "Characterization of Ran-driven cargo transport and the RanGTPase system by kinetic measurements and computer simulation". In: *The EMBO Journal* 22.5 (Mar. 2003), pp. 1088–1100. DOI: 10.1093/emboj/cdg113 (cit. on pp. 2, 4, 12, 13).

[See+03] M. J. Seewald, A. Kraemer, M. Farkasovsky, C. Körner, A. Wittinghofer, and I. R. Vetter. "Biochemical Characterization of the Ran–RanBP1–RanGAP System: Are RanBP Proteins and the Acidic Tail of RanGAP Required for the Ran-RanGAP GTPase Reaction?" In: *Molecular and Cellular Biology* 23.22 (Nov. 2003), pp. 8124–8136. DOI: 10.1128/mcb.23.22.8124-8136.2003 (cit. on p. 5).

[RM05] G. Riddick and I. G. Macara. "A systems analysis of importin-α–β mediated nuclear protein import". In: *Journal of Cell Biology* 168.7 (Mar. 2005), pp. 1027–1038. DOI: 10.1083/jcb.200409024 (cit. on p. 4).

[YM06] W. Yang and S. M. Musser. "Nuclear import time and transport efficiency depend on importin β concentration". In: *Journal of Cell Biology* 174.7 (Sept. 2006), pp. 951–961. DOI: 10.1083/jcb.200605053 (cit. on p. 7).

[ZAH13] J. Zienkiewicz, A. Armitage, and J. Hawiger. "Targeting Nuclear Import Shuttles, Importins/Karyopherins alpha by a Peptide Mimicking the NFκB1/p50 Nuclear Localization Sequence". In: *JAHA* 2.5 (Sept. 2013). DOI: 10.1161/jaha.113.000386 (cit. on p. 7).

[Wüh+14] M. Wühr, R. M. Freeman, M. Presler, M. E. Horb, L. Peshkin, S. P. Gygi, and M. W. Kirschner. "Deep Proteomics of the Xenopus laevis Egg using an mRNA-Derived Reference Database". In: *Current Biology* 24.13 (July 2014), pp. 1467–1475. DOI: 10.1016/j.cub.2014.05.044 (cit. on p. 7).

[Kır+15] K. Kırlı, S. Karaca, H. J. Dehne, M. Samwer, K. T. Pan, C. Lenz, H. Urlaub, and D. Görlich. "A deep proteomics perspective on CRM1-mediated nuclear export and nucleocytoplasmic partitioning". In: *eLife* 4 (Dec. 2015). DOI: 10.7554/elife.11466 (cit. on p. 8).

[NPW19] T. Nguyen, N. Pappireddi, and M. Wühr. "Proteomics of nucleocytoplasmic partitioning". In: *Current Opinion in Chemical Biology* 48 (Feb. 2019), pp. 55–63. DOI: 10.1016/j.cbpa.2018.10.027 (cit. on p. 7).

[Hof20] J.-H. S. Hofmeyr. "Kinetic modelling of compartmentalised reaction networks". In: 197 (Nov. 2020), p. 104203. DOI: 10.1016/j.biosystems.2020.104203 (cit. on p. 5).

[KKL21] J. Kalita, L. E. Kapinos, and R. Y. H. Lim. "On the asymmetric partitioning of nucleocytoplasmic transport – recent insights and open questions". In: *Journal of Cell Science* 134.7 (Apr. 2021). DOI: 10.1242/jcs.240382 (cit. on pp. 5, 7, 8, 14).

List of codes

	page	https://github.com/numpde/nct1/tree/ ...
#1	p.2	main/code/20210225-GSR/v1
#2	p.3	main/code/20210407-Rearrangement
#3	p.3	main/code/20210225-GSR/v2
#4	p.5	main/code/20210403-StickyPore/c_rangap-sequence
#5	p.6	main/code/20211018-Appli

‘

3 Appendix

3.1 Minimal Ran gradient system

Here we recapitulate the minimal Ran gradient system from [GSR03, Fig. 2], cf. §2.1. The following account for the cytoplasmic species. Here, $[\dots]$ abbreviates the (cytoplasmic) concentration of the complex $\mathsf{RanBP1 \cdot Ran \cdot GTP}$. Ex is an additional potentially useful flux of nuclear $\mathsf{Ran \cdot GTP}$ to cytoplasmic $\mathsf{Ran \cdot GDP}$, set by default to zero.

$$\frac{\mathrm{d}}{\mathrm{d}t}[\mathsf{Ran \cdot GDP}]_{\mathrm{cyt}} = \mathsf{F_{Ran \cdot GDP}} \frac{V_{\mathrm{nuc}}}{V_{\mathrm{cyt}}} + \mathsf{GAP} + \mathsf{GAP_{RanBP1}} + \mathsf{Ex} \frac{V_{\mathrm{nuc}}}{V_{\mathrm{cyt}}} \tag{12a}$$

$$\frac{\mathrm{d}}{\mathrm{d}t}[\mathsf{Ran \cdot GTP}]_{\mathrm{cyt}} = \mathsf{F_{Ran \cdot GTP}} \frac{V_{\mathrm{nuc}}}{V_{\mathrm{cyt}}} - \mathsf{GAP} - k_{\mathrm{on}}^{\mathrm{rbp}}[\mathsf{RanBP1}][\mathsf{Ran \cdot GTP}]_{\mathrm{cyt}} + k_{\mathrm{off}}^{\mathrm{rbp}}[\dots] \tag{12b}$$

$$\frac{\mathrm{d}}{\mathrm{d}t}[\mathsf{RanBP1 \cdot Ran \cdot GTP}] = -\mathsf{GAP_{RanBP1}} + k_{\mathrm{on}}^{\mathrm{rbp}}[\mathsf{RanBP1}][\mathsf{Ran \cdot GTP}]_{\mathrm{cyt}} - k_{\mathrm{off}}^{\mathrm{rbp}}[\dots] \tag{12c}$$

The following account for the nuclear species. As in [GSR03], E denotes free $\mathsf{RCC1}$.

$$\frac{\mathrm{d}}{\mathrm{d}t}[\mathsf{Ran \cdot GDP}]_{\mathrm{nuc}} = -\mathsf{F_{Ran \cdot GDP}} + r_8[\mathsf{IntC}] - r_1[\mathsf{E}][\mathsf{Ran \cdot GDP}]_{\mathrm{nuc}} \tag{13a}$$

$$\frac{\mathrm{d}}{\mathrm{d}t}[\mathsf{Ran \cdot GTP}]_{\mathrm{nuc}} = -\mathsf{F_{Ran \cdot GTP}} + r_4[\mathsf{IntA}] - r_5[\mathsf{E}][\mathsf{Ran \cdot GTP}]_{\mathrm{nuc}} - \mathsf{Ex} \tag{13b}$$

The nucleotide-exchange reaction $\mathsf{Ran \cdot GDP + GTP} \rightleftharpoons \mathsf{Ran \cdot GTP + GDP}$ is catalyzed by $\mathsf{RCC1}$. It is modeled as in [Kle+95b, Fig. 6] / [GSR03, Fig. 1] with three intermediates. Note that it depends on the availability of GDP and GTP.

$$\frac{\mathrm{d}}{\mathrm{d}t}[\mathsf{IntA}] = -(r_4 + r_6)[\mathsf{IntA}] + r_5[\mathsf{E}][\mathsf{Ran \cdot GTP}]_{\mathrm{nuc}} + r_3[\mathsf{GTP}][\mathsf{IntB}] \tag{14a}$$

$$\frac{\mathrm{d}}{\mathrm{d}t}[\mathsf{IntB}] = r_6[\mathsf{IntA}] + r_2[\mathsf{IntC}] - (r_3[\mathsf{GTP}] + r_7[\mathsf{GDP}])[\mathsf{IntB}] \tag{14b}$$

$$\frac{\mathrm{d}}{\mathrm{d}t}[\mathsf{IntC}] = -(r_2 + r_8)[\mathsf{IntC}] + r_1[\mathsf{E}][\mathsf{Ran \cdot GDP}]_{\mathrm{nuc}} + r_7[\mathsf{GDP}][\mathsf{IntB}] \tag{14c}$$

Constraints on the total concentration:

$$\text{Free RCC1}: \qquad [\mathsf{E}] = \mathsf{RCC1_{total}} - ([\mathsf{IntA}] + [\mathsf{IntB}] + [\mathsf{IntC}]) \tag{15a}$$

$$\text{Free RanBP1}: \qquad [\mathsf{RanBP1}] = \mathsf{RanBP1_{total}} - [\mathsf{RanBP1 \cdot Ran \cdot GTP}] \tag{15b}$$

Gradient-driven fluxes from the nucleus to the cytoplasm:

$$\mathsf{F_{Ran.GTP}} = D_{\mathsf{Ran \cdot GTP}} \left([\mathsf{Ran \cdot GTP}]_{\mathrm{nuc}} - [\mathsf{Ran \cdot GTP}]_{\mathrm{cyt}}\right) \tag{16a}$$

$$\mathsf{F_{Ran.GDP}} = D_{\mathsf{Ran \cdot GDP}} \left([\mathsf{Ran \cdot GDP}]_{\mathrm{nuc}} - [\mathsf{Ran \cdot GDP}]_{\mathrm{cyt}}\right) \tag{16b}$$

RanGAP hydrolyzes the γ-phosphate of $\mathsf{Ran \cdot GTP}$. This is more efficient when $\mathsf{Ran \cdot GTP}$ is bound to $\mathsf{RanBP1}$ [Bis+95], reducing the IC50 seven-fold [GSR03, Table I, p. 1091].

$$\mathsf{GAP} = k_{\mathsf{GAP}}[\mathsf{RanGAP}]/(1 + K_{\mathsf{GAP}}/[\mathsf{Ran \cdot GTP}]_{\mathrm{cyt}}) \tag{17a}$$

$$\mathsf{GAP_{RanBP1}} = k'_{\mathsf{GAP}}[\mathsf{RanGAP}]/(1 + K'_{\mathsf{GAP}}/[\mathsf{RanBP1 \cdot Ran \cdot GTP}]) \tag{17b}$$

To determine the dynamic capacity Ex at steady-state we introduce the additional equation:

$$\frac{\mathrm{d}}{\mathrm{d}t}\mathsf{Ex} = k_{\mathsf{Ex}}\,[\mathsf{Ran \cdot GTP}]_{\mathrm{nuc}}, \quad k_{\mathsf{Ex}} := 10\,\mathrm{s}^{-2}, \quad \text{initial} \quad \mathsf{Ex} := 0\,\mu\mathrm{M\,s}^{-1}. \tag{18}$$

(12a)	$V_{\text{nuc}} = 1.2\,\text{pl}, \quad V_{\text{cyt}} = 1.8\,\text{pl}$	[GSR03, Table II]
(12a)	initial condition $[\mathsf{Ran}\cdot\mathsf{GDP}]_{\text{cyt}} = 5\,\mu\text{M}$	[GSR03, Table II]
(12b)–(12c)	$k_{\text{on}}^{\text{rbp}} = 0.3\,\mu\text{M}^{-1}\,\text{s}^{-1}, \quad k_{\text{off}}^{\text{rbp}} = 4\times10^{-4}\,\text{s}^{-1}$	[GSR03, Supp. Table A]
(13a)–(14c)	$r_1 = 74\,\mu\text{M}^{-1}\,\text{s}^{-1}, \quad r_8 = 55\,\text{s}^{-1}$ $r_7 = 11\,\mu\text{M}^{-1}\,\text{s}^{-1}, \quad r_2 = 21\,\text{s}^{-1}$ $r_3 = 0.6\,\mu\text{M}^{-1}\,\text{s}^{-1}, \quad r_6 = 19\,\text{s}^{-1}$ $r_5 = 100\,\mu\text{M}^{-1}\,\text{s}^{-1}, \quad r_4 = 55\,\text{s}^{-1}$	[GSR03, Supp. Table A] [Kle+95b, Fig. 6]
(14a)–(14c)	$[\mathsf{GTP}] = 500\,\mu\text{M}, \quad [\mathsf{GDP}] = 1.6\,\mu\text{M}$	[GSR03, Table II]
(15a)	$\mathsf{RCC1}_{\mathsf{total}} = 0.7\,\mu\text{M}$	[GSR03, Supp. Table B]
(15b)	$\mathsf{RanBP1}_{\mathsf{total}} = 2\,\mu\text{M}$	[GSR03, Fig. 4]
(16a) (16b)	$D_{\mathsf{Ran}\cdot\mathsf{GTP}} = 0.03\,\text{s}^{-1}$ $D_{\mathsf{Ran}\cdot\mathsf{GDP}} = 0.12\,\text{s}^{-1}$	[GSR03, Table II]
(17a)	$k_{\mathsf{GAP}} = 10.6\,\text{s}^{-1}, \quad K_{\mathsf{GAP}} = 0.7\,\mu\text{M}$	[GSR03, Supp. Table A]
(17b)	$k'_{\mathsf{GAP}} = 10.8\,\text{s}^{-1}, \quad K'_{\mathsf{GAP}} = 0.1\,\mu\text{M}$	[GSR03, Table I]
(17a)–(17b)	cytoplasmic $[\mathsf{RanGAP}] = 0.7\,\mu\text{M}$	[GSR03, Table II / ST B]

Table 2: Constants for the "standard simulation condition" of §2.1 at 25 °C. Except for (12a), all species are initialized to zero at $t = 0$.

Condition	Affected parameters	Nuclear RanGTP, µM	Cytoplasmic RanGTP, nM	Dynamic capacity, µM/s
"Standard"	See Table 2	4.26 (4.3)	7.75 (7.7)	0.59 (0.60)
Omission of RanBP1	$\mathsf{RanBP1}_{\mathsf{total}} := 0$	4.27 (4.3)	8.13 (8.1)	0.59 (0.60)
200% RCC1	$\mathsf{RCC1}_{\mathsf{total}}$	3.95 (4.0)	7.17 (7.1)	0.59 (0.60)
50% RCC1	$\mathsf{RCC1}_{\mathsf{total}}$	4.31 (4.3)	7.82 (7.7)	0.58 (0.60)
10% RCC1	$\mathsf{RCC1}_{\mathsf{total}}$	3.59 (3.6)	6.50 (6.4)	0.46 (0.48)
1% RCC1	$\mathsf{RCC1}_{\mathsf{total}}$	1.40 (1.4)	2.52 (2.5)	0.075 (0.08)
GTP:GDP = 500:0	$[\mathsf{GDP}] := 0\,\mu\text{M}$	4.80 (4.8)	8.72 (8.6)	0.59 (0.60)
GTP:GDP = 500:50	$[\mathsf{GDP}] := \frac{1}{10}[\mathsf{GTP}]$	0.98 (0.8)	1.76 (1.5)	0.57 (0.58)
GTP:GDP = 500:500	$[\mathsf{GDP}] := [\mathsf{GTP}]$	0.12 (0.12)	0.22 (0.21)	0.34 (0.34)
Saturating NTF2	$D_{\mathsf{Ran}\cdot\mathsf{GDP}} := 0.48\,\text{s}^{-1}$	5.12 (5.1)	9.32 (9.2)	2.18 (2.2)
No NTF2	$D_{\mathsf{Ran}\cdot\mathsf{GDP}} := D_{\mathsf{Ran}\cdot\mathsf{GTP}}$	2.55 (2.5)	4.60 (4.5)	0.15 (0.16)
200% RanGAP	$[\mathsf{RanGAP}]$	4.27 (4.3)	3.95 (3.9)	0.59 (0.60)
50% RanGAP	$[\mathsf{RanGAP}]$	4.26 (4.3)	14.9 (14)	0.59 (0.60)
50% permeability	$D_{\mathsf{Ran}\cdot\mathsf{GTP}}$	4.91 (4.9)	4.44 (4.4)	0.59 (–)
200% permeability	$D_{\mathsf{Ran}\cdot\mathsf{GTP}}$	3.41 (3.4)	12.4 (12.3)	0.59 (–)
400% permeability	$D_{\mathsf{Ran}\cdot\mathsf{GTP}}$	2.46 (2.5)	18.0 (17.8)	0.59 (–)

Table 3: Steady-state concentrations for the simulation scenarios from [GSR03, Table II/III], with their results shown in brackets. Value for $D_{\mathsf{Ran}\cdot\mathsf{GDP}}$ is from [GSR03, Fig. 3].

4 TODO

TODOs:

1. p.1. hydrolysis rate!?
2. p.1. what is NCT
3. p.1. who is involved – transport receptors
4. p.1. why these transport recp
5. p.1. models
6. p.1. contsrut atrificial cells to reproduce a minimalistic NCT system, with the minimal reasonable number of players and to explain observations in vivo showing down or upregulation of certain species
7. p.1. the computatino al model, in turn, closely resembles the design of the artificial cell
8. p.1. here we want to prove that with those players of NCT, the essential observations from are reproduced
9. p.1. role
10. p.1. sys with compartments
11. p.1. visual distribution assuming simple system
12. p.1. ImpBeta = KapBeta1
13. p.2. simplify:
14. p.2. do they have a steady-state result
15. p.2. kinetic behavior of Imp, in addition to cargo and ran
16. p.2. no NE
17. p.2. we look at steady-state
18. p.3. fluxes in Fig 1
19. p.5. cf [KKL21] citing [Kle+95a] or [Kle+95b]
20. p.5. explain initial/final/steady-state
21. p.5. picture
22. p.6. on CAS
23. p.7. refs for those numbers

24. p.7. paralogs?
25. p.7. [unpublished]
26. p.8. link gene
27. p.8. rerun
28. p.8. complete section
29. p.8. :
30. p.8. :
31. p.8. artificial cell should reproduce these
32. p.9. HIGH NPC